УДК 621.762.55:544.6.018.49:621.762

Nanostructured samaria-doped ceria with improved grain-boundary conductivity via SPS and post-SPS annealing

I. Solodkyi, A. Borodianska[1], O. Vasylkiv[1, 2]

National Technical University of Ukraine "KPI", Kyiv,
e-mail: evgen.solodky@gmail.com

[1]Institute for Problems in Materials Science NASU, Kiev

[2]National Institute for Materials Science Tsukuba, Ibaraki, Japan

The 90 nm grained $Ce_{0,8}Sm_{0,2}O_{1,9}$ (SDC) ceramic with relative density of 97% was consolidated via SPS at 1050—1150 °C. The total conductivity values of 0,0079—0,0115 S/cm at 600 °C were obtained. A new approach to improve the grain-boundary conductivity of SDC nano-ceramic has been suggested. The applying of post-SPS low-temperature annealing enabled to decrease the grain-boundary resistance for 1/3, just slight increase in average grain size which avoid increasing of bulk resistance and as a result increase the total conductivity for almost 50%. In addition the SPS followed with post-SPS annealing was shown to be very useful in precise manipulation by the grain size/grain boundary quality/ceramic density, which in turn allow significant property enhancement of nanostructured SDC solid electrolytes.

***Keywords**: solid electrolyte, ionic (electric) conductivity, SPS, post-SPS annealing, grain boundary.*

Introduction

Solid oxide fuel cells (SOFC) have attracted vigorous attention due to several important advantages such as the use of a wide variety of acceptable fuels, appropriate durability and potential efficiency, and development of green technologies [1—5]. The cubic fluorite structured ceria doped with trivalent rare earth elements are considered as advanced oxygen ion conductors. Upon doping with trivalent elements in CeO_2 lattice, the oxygen vacancies are created in order to maintain the charge neutrality of the materials.

Recently, cerium oxide based doped with different dopants [6] have attracted a great interest as a promising solid electrolytes for SOFCs. There are many studies dedicated to identifying the optimal composition of the ceria based electrolytes [7—9]. $Ce_{0,8}Sm_{0,2}O_{1,9}$ is the optimal composition for samarium-doped ceria (SDC) solid electrolyte, which gives the currently highest ionic conductivity. However, till now the influence of grain size and microstructure on the ionic transport properties of these nanocrystalline doped ceria electrolytes in the fairly intermediate temperature range is not clear. Currently, enormous efforts are being made to understand the electrolytic properties of nanoscale ceria based materials for application purpose [8, 10—13].

SDC powder have been successfully prepared by hydrothermal method, providing low-temperature preparation and morphological control in nanosize particles of uniform crystallite dimension [8, 9, 12, 14—16].

It is well known that in the polycrystalline ceria based electrolytes, the impurities such as Si segregate at grain boundaries and form thin blocking layers within the grain boundary network [17—19], which affect the grain

© I. Solodkyi, A. Borodianska, O. Vasylkiv, 2013

boundary conductivity. One way of reducing the larger contribution of segregated impurities is to reduce the grain size to nanoscale region. In such case the total volume of grain boundaries per unit volume increase and the impurities more or less uniformly spread over a large interfacial area [20].

Furthermore, in order to significantly enhance the ionic conductivity, it is necessary to accentuate rapid transport mechanisms [21]. This appears to be possible when the material microstructure is in the nanometer range due to the dominant role of the grain boundary and surface effects, which can exhibit orders of magnitude greater diffusivity than the lattice [21].

It is known that spark plasma sintering (SPS) is highly efficient method for obtaining nano-grain ceramic of different compositions [11, 18—28]. In recent decade the SPS method has received huge attention due to its ability to consolidate a wide variety of difficult-to-sinter materials at low temperatures within a short processing time [12, 13, 22—31].

Up to now, many authors have reported both advantages and disadvantages of SPS method for consolidation the solid electrolytes. One of advantage of SPS is ability to alleviate the harmful effect of contaminants on the overall conductivity, especially on grain boundary conductivity [32]. According to Khor et al. [32] it is possible due to the unique sintering features of SPS with the rapid densification rates. In addition, in comparison with conventional sintering, spark plasma sintering is not only minimizing the processing time from several hours to several minutes. It is also significantly reduce the grain boundary resistance of different electrolytes. For example this is true for silica-containing YSZ electrolyte [33]. Moreover, SPS treatment significantly affects the properties of the sintered material due to the number of features well addressed in ref. [22].

According to the number of reports [10, 12, 23, 28, 34], the significant disadvantage of the rapid SPS treatment of nanostructured ceramics and composites, is underdeveloping of grain-boundary framework. It can be explained by very fast heating and short dwell time [10, 12, 28]. This drawback becomes even more important in case of such materials as the SDC solid electrolyte. For example, Guo et al. [35] showed that the grain boundary resistivity in high purity yttria-doped ceria is still 2—7 order of magnitude higher than the bulk resistivity. The contribution of grain-boundary resistance is significant for this and similar solid electrolytes, and thereby *the improvement of grain-boundary conductivity becomes extremely important.* This improvement becomes crucial if ceramic is nanostructured.

The comprehensive meticulous analysis of number of studies allowed to conclude that applying of rapid SPS consolidation results in producing the ceramic with homogeneous grain size distribution but simultaneously with under-developed grain-boundary framework. This main drawback of rapid densification processes leads to inaccessibility of the potentially high performance in a great number of fine-grained ceramics and composites.

Here in this study we will show the results of our efforts in stabilization/homogenization of grain-boundary framework in SPS-derived SDC nanoceramic by applying of post-SPS annealing. Therefore the first aim of present work was an optimization of spark plasma consolidation technique to obtain dense nanostructured SDC ceramic with high total conductivity. Surprisingly that up to now, there is no report on SPS consolidation of SDC ceramic. Stabilization/homogenization of grain boundaries and thereby improvement of

the total conductivity of SDC ceramic is the second- main aim of this work. For this reason, the variation of grain-boundary resistance as a function of post-SPS annealing was analyzed and addressed.

Experimental

The solid solution $Ce_{1-x}Sm_xO_{2-x/2}$ (x = 0,20) was synthesized and crystallized under hydrothermal conditions as reported previously [11]. This preparation method provided a powder with the primary crystallite size in the range of 7—11 nm and aggregates with size distribution of 35—59 nm which was calculated from TEM images [12] After hydrothermal synthesis and subsequent calcination, the powder had the cubic fluorite structure of cerium oxide which agrees with the standard JCPDS (89-8436). No secondary phase was identified from the XRD pattern for the as-prepared and annealed samples.

The spark plasma sintering system Dr. Sinter Model SPS-1050, SPS-Syntex, Japan was used for consolidation of SDC powder. The $Ce_{0,8}Sm_{0,2}O_{1,9}$ powder samples with constant weigh of 0,8 g were loaded into the graphite die and plunger unit (10 mm in diameter), which then was placed inside the SPS apparatus. Graphite foils (Grafoil) were used to isolate the specimen from the die and the plunger surfaces. The temperature was controlled by an optical pyrometer focused on the non-through hole located at the surface of the graphite die. The sintering experiments were conducted in Ar flowing atmosphere. The sintering temperature was in the range of 1000—1150 °C for hold time of 6—15 min at the maximum pressure of 150 MPa. The heating rates were 400 and 500 °C/min. In order to decrease the radial temperature gradient during sintering an insulating felt were mounted on the die. In addition, twelve SPSed samples of three series S1, S2 and S3 were annealed at 1000 °C in air for 4, 10, 20 and 30 h. The samples ID were chosen as follows: S1-4, S1-10, S2-4, and so on.

The crystal characteristics of the samarium doped cerium oxide were investigated by using powder X-ray diffraction in a reflection mode on a Bruker AXS diffractometer (D8 Advance, Germany) fitted with Cu-tube (CuK_α-radiation). The crystal structure of the materials was refined by Rietveld analysis with a fundamental parameter approach in the program TOPAS [36, 37]. The starting model for refinement was based on the crystallographic data published for cerium oxide [38]. Microstructure observations and local compositional analysis measurements were taken with JEOL JEM-2100F and JEOL JSM 7001F (Japan) electronic microscopes equipped with energy dispersive systems. Particle size distribution was determined by randomly selecting 200 particles in SEM pictures using software “SIAMS”. Densities of all sintered samples were measured by using the Archimedes method with distilled water as the immersion medium. The theoretical density calculated from the X-ray diffraction patterns was 7,15 g/cm^3. For conductivity characterization by complex impedance spectroscopy, Pt-paste electrodes were applied and dried in the air at 900 °C for 0,5 h. Measurements were done in the air at various temperatures. An impedance analyzer (Hewlett Packard HP 4194A) working in the range of 100 Hz—15 MHz was used.

Result and discussion

Characteristics and electrical properties of SDC ceramic after SPS

The $Ce_{0,8}Sm_{0,2}O_{1,9}$ ceramic with 0,07—0,12 μm grain size and relative density of more than 97% has been successfully obtained by using SPS method.

T a b l e 1. Characteristics of SDC bulk ceramic consolidated by SPS and improved by post-SPS annealing

Sample ID	Tempe-ratyre, °C	Hold time, h	Relative densoty, %					Grain size diatribution, μm				
			SPS only	Post-SPS annealing at 1000 °C				SPS only	After post-SPS annealing at 1000 °C			
				4 h	10 h	20 h	30 h		4 h	10 h	20 h	30 h
S1	1050	0,1	97,2	97,3	97,7	98,3	98,4	0,07—0,11	0,08—0,14	0,15—0,23	0,24—0,31	0,35—0,66
S2	1050	0,25	97,8	97,9	98,1	98,9	99,0	0,07—0,12	0,08—0,15	0,16—0,23	0,23—0,34	0,39—0,71

As expected, the average grain sizes of 90 and 95 nm and relative densities of 97,2 and 97,8% gradually increase with increasing the holding time from 6 to 15 min at 1050 °C, respectively (table 1). The pellet sintered at 1150 °C with no soaking has the relative density of 97,6% with an average grain size of 95 nm. However, it can be seen that all of these samples have almost the similar density and grain size distribution. Thus, SDC ceramic samples which differ only in the sintering temperature and holding time were prepared with the purpose for better understanding the nature of the grain boundaries after SPS sintering.

In fig. 1 are presented XRD patterns of the as synthesis powder (P) and sample (S1) SPSed at 1050 °C with 6 min holding. We choose the S1 sample due to its best total conductivity (table 2). Besides the two other SPSed samples (S2 and S3) have almost identical XRD patterns. These results indicate that the doped ceria samples have formed ceria-based solid solutions with fluorite-type structure, which was obtained during the calcination process and subsequent proper crystallization after sintering and annealing. Therefore, the results are in good agreement with the standard JCPDS (89-8436). No secondary phase was identified from the XRD pattern for the as-prepared powder and bulk samples consolidated by SPS. Moreover, the peak broadening (fig. 1 (P)) indicated that the powder consisted of superfine primary crystallites. The typical effect of grains growth during SPS on the crystal system is shown in fig. 1 (S1). The width of the XRD peaks decreased after sintering. However the width of the peaks after SPS still significant, and suggests that SPSed ceramic remained nanograined.

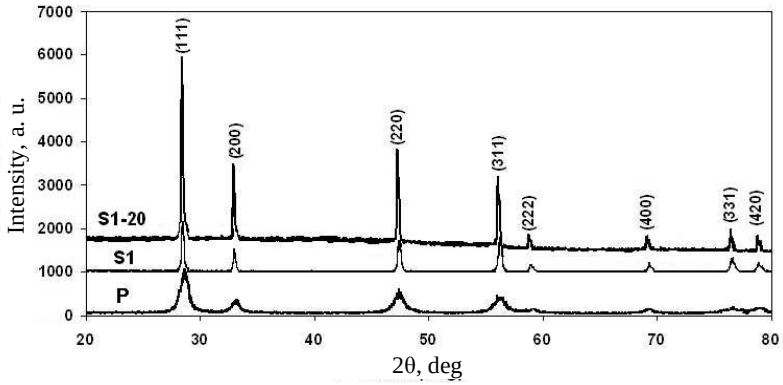

Fig. 1. X-ray diffraction patterns of samaria-doped ceria ceramics (P) as synthesis powder, (S1) sintered by SPS at 1050 °C 6 min holding and (S1-20) the same sample but after annealing 20 hours.

The effect of SPS parameters on the conductivity of consolidated polycrystalline SDC samples was studied and addressed. As shown in table 2, the SDC solid electrolyte with the electrical conductivity of 0,0079 to 0,0115 S/cm at 600 °C was obtained at various SPS regimes. All samples showed very similar average grain size. The highest electrical conductivity value of 0,0115 S/cm was shown at 600 °C by the $Ce_{0,8}Sm_{0,2}O_{1,9}$ ceramic sample with the grain size of 0,07—0,11 μm and the relative density of 97,2%. This S1 sample was SPSed at 1050 °C for 6 min. The prolonged from 6 to 15 min holding at 1050 °C resulted in slight increasing of relative density to 97,8%. However, this longer holding did not lead to significant grain growth as well as to any significant increase in total conductivity at the temperature interval of 300—600 °C. The value of total conductivity at 600 °C for the sample S2 SPSed at 1050 °C for 15 min was 0,0114 S/cm. On the other hand, the increase of sintering temperature up to 1150 °C with no holding leaded to obtaining sample S3 with grain size of 0,07—0,012 μm and a relative density of 97,5%, but also did not cause any increase in total conductivity (value of 0,0079 for S3 sample). The total conductivity of the sample S2 increased only after the operation temperature exceeded the level of 600 °C (fig. 2). However, this increase in total conductivity above the 600 °C should be explained by the appearance of electronic conductivity in the sample due to the introducing of electrons into the samples [39]. Thus, according to fig. 2 the slope of the temperature dependence of total conductivity of SPSed SDC solid electrolytes became sharper due to the lower activation energy of electronic conductivity. For example, the activation energy for the sample S1 at the temperature range of 300—600 °C was almost 0,89 eV. However it significantly decreases to 0,59 eV at an operation temperature of 650—800 °C. The similar behavior was observed for all SPSed samples (fig. 2). These data allows assumption that prolonged from 6 to 15 min holdings at 1050 °C did not cause a significant improvement in total conductivity of $Ce_{0,8}Sm_{0,2}O_{1,9}$ electrolytes.

The ceramic samples S1, S2, S3 with almost same grain size in the range of 0,07 to 0,12 μm and relative density of 97,2 to 97,8% showed total conductivity values of 0,0115, 0,0114, 0,0079 S/cm (at 600 °C), respectively (tables 1 and 2). The samples S1 and S2 have slightly different value of total conductivity however this difference is less than 1% and can be neglect. In contrast

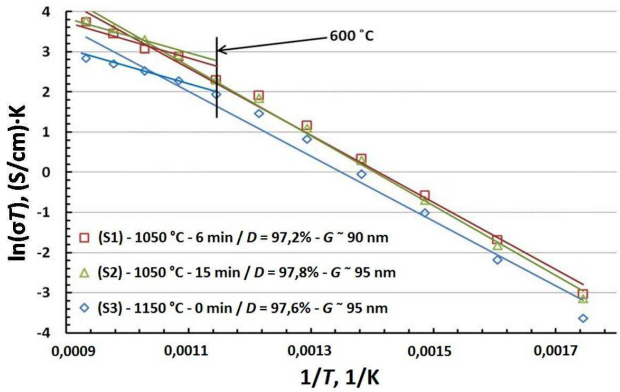

Fig. 2. Temperature dependence of total conductivity for SDC solid electrolytes SPSed under the different conditions.

T a b l e 2. Total conductivity of SDC bulk ceramic consolidated by SPS and using post-sintering annealing

Sample ID	Tempe-rature of SPS, °C	SPS hold time, h	Total conductivity at 600 °C, S/cm				
			SPS only	SPS and post-SPS annealing at 1000 °C			
				4 h	10 h	20 h	30 h
S1	1050	0,1	0,0115	0,0123	0,0162	0,0169	0,0167
S2	1050	0,25	0,0114	0,0121	0,0157	0,0159	0,0156
S3	1150	—	0,0079	0,0081	0,0089	0,0096	0,0092

the total conductivity of the samples S1 and S2 differ for about 45% if to compare with S3 sample. This may be explained by the microstructural differences between the S1 and S2 electrolytes SPSed at 1050 °C and S3 electrolyte consolidated at a higher temperature of 1150 °C with no holding. Higher sintering temperature allowed to obtain ceramic with similar relative density of 97,5% and an average grain size of 95 nm. However, grain boundary framework remained underdeveloped due to the very short consolidation time and absence of isothermal homogenization. It was found that the best low-temperature conductivity of 0,0115 S/cm is observed for bulk SDC S1 specimen with finest average grain size, consolidated at 1050 °C with 6 min holding (fig. 2).

Properties of SDC ceramic after post-SPS annealing

It can be seen from table 2 that in general, the samples prepared by SPS do not exhibit extraordinary electrical properties. Taking into account this result one can conclude that SPS enables consolidation of nanostructured ceramic with desirable grain size and homogeneity. However, simultaneousle, SPSed ceramic, in general, exhibit under-developing of grain-boundary framework and, as a result, do not exhibit extraordinary electrical properties. Here for SPSed $Ce_{0,8}Sm_{0,2}O_{1,9}$, the total conductivity at 600 °C was just 0,0079—0,0115 S/cm even the grains were nanosized and the relative density was 97—98%. This very ordinary result signified the following attempts on homogenization/ improvement of grain boundary framework via manipulating by the post-SPS annealing parameters.

The relative densities and the grain size distribution for samaria-doped ceria samples SPSed only and SPSed with subsequent different-term annealing are collected in table 1. As was expected, the average grain size and density gradually increased from 0,115 to 0,545 μm and from 97,3 to 99,0%, respectively, with increase in post-SPS annealing duration from 4 to 30 hours. If the relative density just slightly increase for only 1% with 20 h annealing at 1000 °C, the average grain size of all samples simultaneously increased for almost 3 times. More prolonged 30 h annealing in general cause the grains coarsening to 0,545 μm (table 1). The grain growth dynamics for all three sample series is almost the same. The XRD patterns on fig. 1 (S1, S1-20) shows the typical effect of grains growth during annealing of SDC nanostructured samples. The width of the XRD peaks has decreased after 20 h annealing (S1-20). No secondary phase was identified from the XRD pattern for any SPSed and subsequently shorter or longer term annealed sample (Not shown

here due to similarity). The crystal structure of SDC samples gradually improves from just SPSed (the pattern S1) to SPSed and subsequently annealed for 20 h at 1000 °C (the pattern S1-20).

The total conductivity at 600 °C of $Ce_{0,8}Sm_{0,2}O_{1,9}$ samples of S1 and S2 series increased for just about 6% after 4 h annealing and exceeded the values of 0,0115 and 0,0114 S/cm for samples S1-4 and S2-4 respectively. The more continuous annealing for 10 and 20 hours significantly increased the values of the total conductivity at 600 °C up to 0,0162, 0,0169 S/cm and 0,0157, 0,0159 S/cm for samples S1-10, S2-10 and S1-20, S2-20 respectively. The total conductivities after annealing for 10 and 20 hours in the case of samples S3-10 and S3-20 were 0,0089 and 0,0096 S/cm at 600 °C, respectively. Finally after 30 h post-SPS annealing the samples S1-30, S2-30, S3-30 exhibit the respective values of 0,0167, 0,0156, and 0,0092 S/cm at 600 °C. This last data clearly showed that more prolonged post-SPS annealing lead to a decrease in total conductivity. The comparative analysis of the grain size to relative density dependence from the annealing time (table 1) allows the following preliminary conclusions. The decrease in total conductivity due to the post-SPS annealing for 30 h should be directly associated with a significant grain growth. The highest value of 0,0169 S/cm total conductivity at 600 °C was obtained for the sample S1-20. This value most likely should be attributed to the following factors (1). The effect of longer exposure of 15 min at 1050 °C and a higher sintering temperature of 1150 °C for the sample series S2 and S3, respectively, could hinder the stabilization of grain boundaries during annealing (2). The sample S1 and all samples of this series showed the smallest average grain size along with the high relative density of more than 97% after SPS densification and post-SPS annealing (3). Finally the sample S1 showed the highest total conductivity after SPS itself (table 2).

In order to achieve better understanding of the phenomena which cause increasing of total conductivity of post-SPS annealed SDC samples, the impedance spectra's were also recorded at 500 °C for SPS-derived (S1) and annealed for S1-10, S1-20 and S1-30 samaria-doped ceria solid electrolytes (fig. 3). The temperature of 500 °C is an approximate operating temperature of low-temperature SOFCs with ceria-based solid electrolytes. Also, this temperature allows to separate the bulk and the grain boundary components of resistance. To avoid the overloading of fig. 3, the impedance spectroscopy diagram for S1-4 sample is not shown, since the resistance of the sample did not change significantly after this short-time annealing.

The impedance spectra of SPSed and annealed for 10, 20, and 30 h SDC electrolytes were analyzed on fig. 3. The grain boundary (GB) resistance of S1 and S1-4 samples was detected as 117,7 and 111,4 Ω, respectively. Although the grain boundary resistance almost unchanged after 4 h annealing, the longer term annealing for 10 and 20 h in contrast results in GB resistance significant lowers to 88,3 and 80,5 Ω, respectively. However, it should be emphasized once again that annealing duration of more than 20 h leads to increase in both bulk and grain boundary resistance (S1-30 in fig. 3). This data is well correlated with a significant increase in average grain size, which neglect or totally neutralize the main positive effect of improving the quality (homogenization) of the grain-boundary framework. In addition we can assume from the fig. 3 that the bulk resistance of SDC samples of S1 series remained almost unchanged after 10 and 20 h post-SPS annealing; and slightly increased from

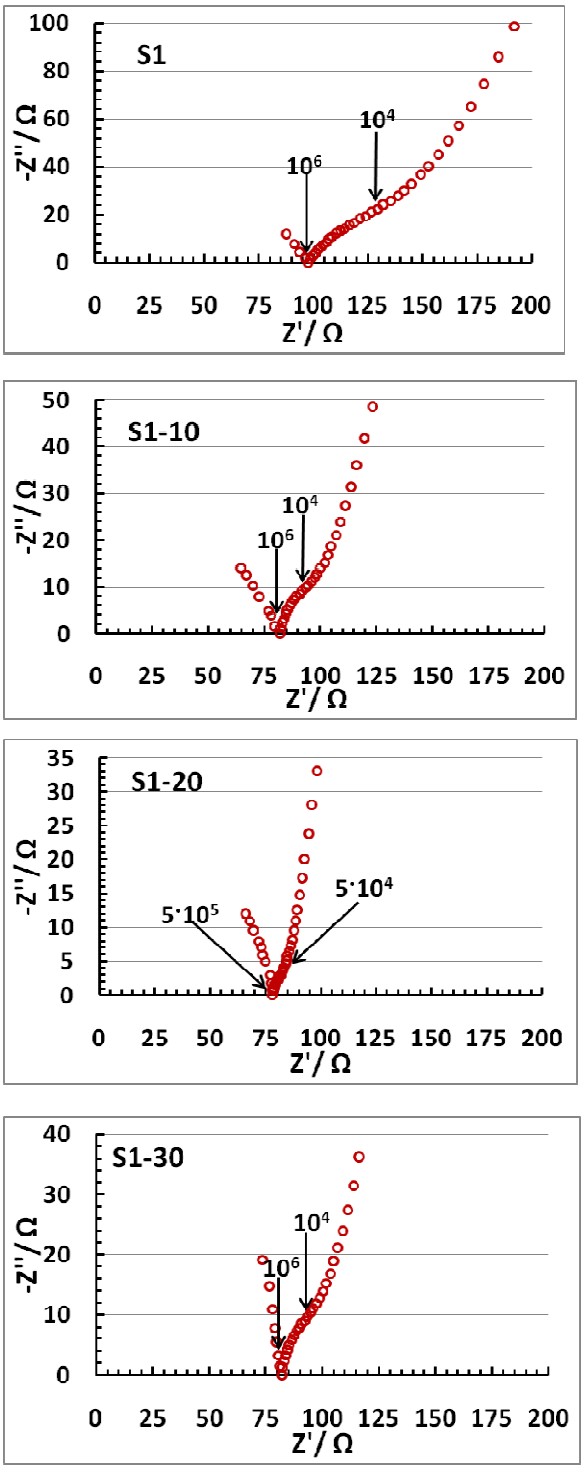

Fig. 3. Impedance spectroscopy diagrams pellets densification by SPS 1050 ˚C at 6 min, measuring temperature 500 ˚C: S1 — without annealing; S1-10 — after annealing 10 h at 1000 ˚C; S1-20 — after annealing 20 h at 1000 ˚C; S1-30 — after annealing 30 h at 1000 ˚C.

76,1 to 79,6 Ω with increasing of an average grain size to 0,505 μm after 30 h post-SPS annealing. Some assumptions can be done on the basis of the above results. The grain boundary resistance reduces due to the positive influence of grain boundary framework homogenization. However, the simultaneous (even relatively low-rate) grain growth negatively influences on the bulk resistance. Due to such superimposing of both positive and negative factors the long-term annealing becomes meaningless**.**

Razavi et al. [40] used two-step sintering of nanocrystalline zirconia powder stabilized with 8% (mol.) yttria which resulted in remarkable enhancement of the electrical conductivity (>95% increase) and suppression of the exaggerated grain growth. This success achieved due to both a significant reduction of the average grain size and stabilization of grain boundaries by long-term soaking at the temperature of 100 to 200 °C lower than the sintering temperature.

Bernard-Granger et al. [13] noted that Moire´ patterns can be seen after SPS. Since dislocations are sources of vacancies, then it became clear that a higher dislocation density promotes the higher ionic conductivity. Then, as higher the Moire´ pattern density, as more significant increase in the total ionic conductivity [13] According to this report the increase in conductivity after annealing also can be explained. Martin et al. [41] reported the increase in conductivity after annealing of samples densificated by pressureless sintering (PLS). The authors explain this in terms of cleaning of grain boundaries and decrease in grain boundary volume with increase in grain size after annealing. Although the increase of electric conductivity with decrease in grain size is well known [42—45].

The results in fig. 4 suggest that along with increase in grain size, the stabilization of grain boundaries after annealing is observed and leads to significant decrease in GB resistance. Earlier, the new method of the grain-boundary conductivity enhancement via pre- and post-sintering heat treatment were suggested for the yttria-stabilized zirconia [46, 47] and gadolinia-doped ceria [48] nanoceramics. These authors improved the grain-boundary conductivity for ceramic with 100—150 ppm of SiO_2 impurity via gathering of siliceous impurity and reducing of the average grain size.

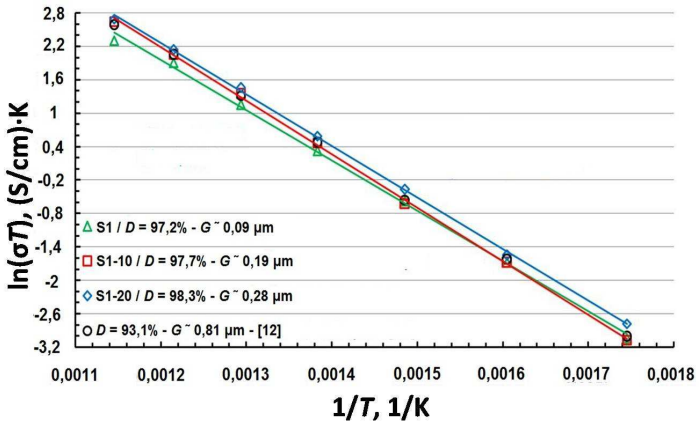

Fig. 4. Temperature dependence of total conductivity for SDC solid electrolytes SPSed (S1) and subsequently annealed at 1000 ˚C for 10 and 20 h (S1-10 and S1-20), and sintered in air.

Thus, the influence of the parameters of SPS and especially subsequent post-SPS annealing on the characteristics and electrical properties of SDC ceramic have not been previously addressed. It can be seen from fig. 4, that the sample with the highest total conductivity measured at low temperatures of 300—600 °C been produced by SPS at only 1050 °C (S1) and exhibited the electrical conductivity of 0,0169 S/cm at 600 °C. Later by applying of post-SPS annealing at 1000 °C for 10 and 20 h, the total conductivity was enhanced by 40% for S1-10 and 47% for S1-20 samples respectively.

Comparing of the above results with the data presented in previous report [11], allows few following conclusions. The proposed technique for consolidation facilitate the obtaining of high-density, with keeping controllably low grain size in the range of 0,1—0,34 μm, and homogeneous grain-boundary framework. SDC ceramic with high relative density of 98% and an average grain size of 0,27 μm was obtained by SPS with subsequent post-SPS annealing in air. The total conductivity of 0,0169 S/cm at 600 °C was obtained in the present study, which is by almost 15% higher in comparison with 93% dense SDC electrolyte of same composition with 0,81 μm average grain size [12] (fig. 4).

The significant enhancement of total conductivity can be attributed to the following reasons: (*i*) suppressing of grain growth due to the rapid SPS consolidation; (*ii*) effect of grain boundary stabilization/homogenization; (*iii*) increase in relative density of bulk ceramic.

Conclusions

The effect of annealing after SPS on the electrical conductivity of polycrystalline cerium-samarium oxide was studied and addressed. It was clarified that high density and fine-grained microstructure are not sufficient for high ionic conductivity. The electric conductivities of fine-grained samaria-doped ceria solid electrolytes were enhanced by low-temperature annealing with aim to homogenize the grain-boundary framework. $Ce_{0.8}Sm_{0.2}O_{1.9}$ solid electrolyte showed the enhanced for almost 50% values of electric conductivity of 0,0162 and 0,0169 S/cm at 600 °C after post-SPS annealing at 1000 °C for 10 and 20 h respectively. The grain boundaries were homogenized which thereby reduced their resistance. More precisely, the grain boundary resistance after 20 h annealing decreased from 117,7 to 80,5 Ω.

Finally the main conclusion should be done that by means of low-temperature SPS and subsequent post-SPS annealing the desirable ratio of grain size to homogeneity of grain boundary framework may be achieve for close to full-dense nanostructured ceramic, which significantly improves its functional characteristics.

1. *Weber A.* Materials and concepts for solid oxide fuel cells / A. Weber, E. Ivers-Tiffee // J. Power Source. — 2004. — **127**. — P. 273—283.
2. *Kurumada M.* Electric conductions in $La_{0,9}Sr_{0,1}GaO_{3-\delta}$ and $La_{0,9}Sr_{0,1}Ga_{0.9}Mg_{0,1}O_{3-\delta}$ / M. Kurumada, H. Hara, F. Munakata // Solid State Ionics. — 2005. — **176**. — P. 245—251.
3. *Gong W.* Performance of intermediate temperature (600—800 °C) solid oxide fuel cell based on Sr and Mg doped lanthanum-gallate electrolyte / W. Gong, S. Gopalan, U. B. Pal // J. of Power Sources. — 2006. — **160**. — P. 305—315.
4. *Lee D.* Preparation and characterization of strontium and magnesium doped lanthanum gallates as the electrolyte for IT-SOFC / D. Lee, J. H. Han, Y. Chun // Ibid. — 2007. — **166**. — P. 35—40.

5. Li Z.—C. Synthesis and characterization of LaSr by steric entrapment synthesis method / Z.—C. Li, H. Zhang, B. Bergman // J. Eur. Ceram. Soc. — 2006. — **26**. — P. 2357— 2364.
6. *Kuharuangrong S.* Ionic Conductivity of Sm, Gd, Dy and Er-doped-Ceria // J. Power Sources. — 2007. — **171**. — P. 506—510.
7. *Huang W.* Properties of sol-gel prepared $Ce_{1-x}Sm_xO_{2-x/2}$ solid electrolytes / W. Huang, P. Shuk and M. Greenblatt // Solid State Ionics. — 1997. — **100**. — P. 23—27.
8. *Fu, Y. P.* Preparation and characterization for solid oxide fuel cells / Y. P. Fu, S. B. Wen, C. H. Lu // J. Amer. Ceram. Soc. — 2007. — **91 (1)**. — P. 127—131.
9. *Dikmen S.* Hydrothermal synthesis and properties of $Ce_{1-x}Gd_xO_{2-\delta}$ solid solutions / S. Dikmen, P. Shuk, M. Greenblatt // Solid State Sci. — 2002. — **4**. — P. 585—590.
10. *Borodianska H.* Nanometric $La_{0,9}Sr_{0,1}Ga_{0,8}Mg_{0,2}O_{3-x}$ ceramic prepared by low-pressure reactive spark-plasma-sintering / H. Borodianska, P. Badica, T. Uchikoshi // J. Alloy. Compd. — 2001. — **509 [5]**. — P. 2535—2539.
11. *Bernard-Granger G.* Spark plasma sintering of a commercially available granulated zirconia powder-II. Microstructure after sintering and ionic conductivity / G. Bernard-Granger, C. Guizard, S. Surble // J. Acta Mater. — 2008. — **56**. — P. 4658.
12. *Solodkyi I.* Effect of grain size on the electrical properties of samaria-doped ceria Solid electrolyte / I. Solodkyi, H. Borodianska, Y. Sakka // J. Nanosci. Nanotechnol. — 2012. — **12 [3]**. — P. 1871—1879.
13. *Bernard-Granger G.* Spark plasma sintering of a commercially available granulated zirconia powder: Comparison with hot-pressing / G. Bernard-Granger, A. Addad, G. Fantozzi // Acta Mater. — 2010. — **58**. — P. 3390—3399.
14. *Inaba H.* Ceria-based solid electrolytes / H. Inaba, H. Tagawa // Solid State Ionics. — 1996. — **83**. — P. 1—16.
15. *Tianshu Z.* Ionic conductivity in the CeO_2—Gd_2O_3 prepared by oxalate co-precipitation / Z. Tianshu, P. Hing, H. Huang // Solid State Ionics. — 2002. — **148**. — P. 567—573.
16. *Vasylkiv O.* Hydroxide synthesis, colloidal processing and sintering of nano-size 3Y—TZP powder / O. Vasylkiv, Y. Sakka // Scripta Mater. — 2001. — **44**. — P. 2219—2223.
17. *Zhang T. S.* Different conduction behaviors of grain boundaries in SiO_2-containing 8YSZ and CGO20 electrolytes / T. S. Zhang, J. Ma, Y. Z. Chen // Solid State Ionics. — 2006. — **177**. — P. 1227—1235.
18. *Zhang T. S.* Intermediate-temperature ionic conductivity of ceria-based solid solutions as a function of gadolinium and silica contents / T. S. Zhang, J. Ma, Y. Z. Chen // Solid State Sci. — 2004. — **6**. — P. 565—572.
19. *Guo X.* Blocking grain boundaries in yttria-doped and undoped ceria ceramics of high purity / X. Guo, W. Sigle, J. Maier // J. Amer. Ceram. Soc. — 2003. — **86**. — P. 77—87.
20. *Ashok Baral K.* Electrical study and dielectric relaxation behavior in nanocrystalline $Ce_{0,85}Gd_{0,15}O_{2-\delta}$ / K. Ashok Baral, V. Sankaranarayanan // Appl. Phys. A. Material at Intermediate Temperatures. — 2010. — **98**. — P. 367—373.
21. *Kosacki I.* Nanoscale effects on the ionic conductivity / I. Kosacki, C. M. Rouleau, P. F. Becher // Electrochemical and Solid-State Letters. — 2004. — **7**. — P. 459—461.
22. *Borodianska H.* Sintering of $Gd_{20}Ce_{80}O_{1,90}$ Nanopowders / H. Borodianska, O. Vasylkiv, Y. Sakka // J. Nanosci. Nanotechnol. — 2008. — **8**. — P. 3077—3084.
23. *Borodianska H.* Bulk Ti1—xAlxN nanocomposite via spark plasma sintering of nanostructured Ti1—xAlxN—AlN powders / H. Borodianska, T. Ludvinskaya, Y. Sakka // Scripta Mater. — 2009. — **61**. — P. 1020—1023.
24. *Grasso S.* Effects of pressure applicationm on transparency of SPSed alumina / S. Grasso, Y. Sakka, G. Maizza // J. Amer. Ceram. Soc. — 2009. — **92**. — P. 2419—2471.

25. *Grasso S.* Electric current activated/assisted sintering (ECAS) a rewiev of patents / S. Grasso, Y. Sakka, G. Maizza // Sci. Technol. Adv. Mater. — 2009. — **10**. — P. 053001.
26. *Suárez G.* Zirconia nanoceramic via redispersion of highly agglomerated (2,7Y-TZP) nanopowder was synthesized and stored for five years / G. Suárez, H. Borodianska, Y. Sakka // J. Nanosci. Nanotechnol. — 2010. — **10**. — P. 6634—6640.
27. *Vasylkiv O.* Nanoblast Synthesis and Consolidation of $(La_{0,8}Sr_{0,2})(Ga_{0,9}Mg_{0,1})O_{3-\delta}$ under spark plasma sintering conditions / O. Vasylkiv, H. Borodianska, P. Badica // J. Nanosci. Nanotechnol. — 2009. — **9**. — P. 141—149.
28. *Bezdorozhev O.* Tough yttria-stabilized zirconia ceramic by low-temperature spark plasma sintering of long-term stored nanopowders / O. Bezdorozhev, H. Borodianska, Y. Sakka // J. Nanosci. Nanotechnol. — 2011. — **11** [9]. — P. 7901—7909.
29. *Badica P.* Beautiful' unconventional synthesis and processing technologies of superconductors and some other materials / P. Badica, A. Crisan, G. Aldica // Sci. Technol. Adv. Mater. — 2011. — **12**. — P. 013001.
30. *Borodianska H.* Grain boundary diffusion driven spark plasma sintering of nanocrystalline zirconia / H. Borodianska, D. Demirskyi, S. Grasso //Ceram. Internat. — 2012. — **38**. — P. 4385—4389.
31. *Raj R.* Influence of externally imposed and internally generated diffusional creep, sintering and related phenomena in ceramics / R. Raj, M. Cologna, J. S. C. Francis // J. Amer. Ceram. Soc. — 2011. — **94**. — P. 1941—1965.
32. *Chen X. J.* Reducing effect of con-taminants in solid oxide fuel cell electrolyte bys plasma sintering / X. J. Chen, K. A. Khor, S. H. Chan // Adv. in Appl. Ceram. — 2005. — **104** (3). — P. 117—122.
33. *Chen X. J.* Overcoming the effect of blocked in silica-doped yttria-stabilized zirconia (YSZ) / X. J. Chen, K. A. Khor, S. H. Chan // Mater. Sci. Eng. A. — 2004. — **374**. — P. 64—71.
34. *Borodianska H.* Si_3N_4—TiN Nanocomposite by nitration of $TiSi_2$ and consolidation by hot pressing and spark plasma sintering / H. Borodianska, L. Krushinskaya, G. Makarenko // J. Nanosci. Nanotechnol. — 2009. — **9**. — P. 6381—6389.
35. *Guo X.* Blocking grain boundaries in yttria-doped and undoped ceria ceramics of high purity / X. Guo, W. Sigle, J. Maier // J. Amer. Ceram. Soc. — 2003. — **86**. — P. 77—87.
36. *Cheary R. W.* A fundamental parameters approach to X-ray line-profile fitting / R. W. Cheary, A. Coelho // J. of Appl. Crystallography. — 1992. — **25**. — P. 109.
37. TOPAS. Bruker AXS GmbH, Germany, Karlsruhe, 2003.
38. *Varez A.* Structural characterization of $Ce_{1-x}Zr_xO_2$ ($x \leq 1$) samples prepared at 1650 degree by solid state reaction: A combined TEM and XRD study / A. Varez, E. Garcia-Gonzalez, J. Jolly // J. of the European Ceram. Soc. — 2007. — **27**. — P. 3677—3682.
39. *Guo X.* Space charge concept for acceptor-doped zirconia and ceria and experimental evidences / X. Guo, R. Waser // Solid State Ionics. — 2004. — **173**. — P. 63—67.
40. *Hesabi Z. R.* Enhanced electrical conductivity of ultrafine-grained $8Y_2O_3$ stabilized ZrO_2 produced by two-step sintering technique / Z. R. Hesabi, M. Mazaheri, T. Ebadzadeh // J. Alloys Comp. — 2010. — **494**. — P. 362—365.
41. *Martin M. C.* Zirconia as a function of silica content and grain size / M. C. Martin, M. L. Mecartney // Solid State Ionics. — 2003. — **161**. — P. 67—79.
42. *Yan D.* Electrical properties of grain boundaries and size effects in samarium-doped ceria / D. Yan, X. Liu, X. Bai // J. Power Source. — 2010. — **195**. — P. 6486—6490.
43. *Ding D.* Electrical properties of samaria-doped ceria electrolytes from highly active powders / D. Ding, B. Liu, M. Gong // Electrochimica Acta. — 2010. — **55**. — P. 4529—4535.

44. *Abdala P. M.* Enhanced ionic transport in fine- grained scandia-stabilized zirconia ceramics / P. M. Abdala, G. S. Custo, D. G. Lamas // J. Power Sources. — 2010. — **195**. — P. 3402—3406.
45. *Chen M.* Preparation and electrochemical properties of Ni-SDC thin films for IT-SOFC anode / M. Chen, B. H. Kima, Q. Xub // Ceram. Internat. — 2009. — **35**. — P. 1335—1343.
46. *Lee J.-H.* Pt—CeO_x nanocomposite electrocatalyst — An *in situ* electrochemical X-ray absorption fine structure / J.-H. Lee, T. Mori, J.-G. Li // J. Electrochem. Soc. — 2000. — **147**. — P. 2822—2829.
47. *Lee J.-H.* Precursor scavenging of resistive grain-boundary phase in 8% (mol.) ytterbia-stabilized zirconia / J.-H. Lee, T. Mori, J.-G. Li // J. Electrochem. Soc. — 2002. — **149**. — P. 35—40.
48. *Kim D.-S.* Transport properties of solid oxide electrolyte ceramics: a brief review / D.-S. Kim, P.-S. Cho, J.-H. Lee // Solid State Ionics. — 2006. — **177**. — P. 2125—2128.

Підвищення провідності границь зерен наноструктурного церію, легованого самарієм, за рахунок застосування відпалу після спікання методом ИПС

Є. В. Солодкий, Г. Ю. Бородянська, О. О. Васильків

Кераміка $Ce_{0,8}Sm_{0,2}O_{1,9}$ (SDC) з середнім розміром зерна 90 нм та відносною щільністю 97% отримана іскроплазмовим спіканням (ІПС) при температурі 1050—1150 °С. Загальна електрична провідність щільного матеріалу становила 0,0079—0,0115 См/см при 600 °С. Запропоновано новий підхід до поліпшення зернограничної провідності нанокераміки SDC. Застосування низькотемпературного відпалу після спікання методом ІПС дозволило знизити опір границь зерна на 1/3 при незначному збільшенні їх середнього розміру. Показано, що відпал після ІПС є ефективним методом контролю якості границь зерен, розміру зерна та щільності. Це дозволяє підвищити функціональні властивості твердого електроліту SDC.

Ключові слова: *твердий електроліт, іонна (електрична) провідність, ІПС, відпал після ІПС, границя зерна.*

Повышение проводимости границ зерен наноструктурного церия, легированного самарием, за счет применения отжига после спекания методом ИПС

Е. В. Солодкий, А. Ю. Бородянская, О. О. Васылькив

Керамика $Ce_{0,8}Sm_{0,2}O_{1,9}$ (SDC) со средним размером зерна 90 нм и относительной плотностью 97% получена искроплазменным спеканием (ИПС) при температуре 1050—1150 °С. Общая электрическая проводимость плотного материала составила 0,0079—0,0115 См/см при 600 °С. Предложен новый подход к улучшению зернограничной проводимости нанокерамики SDC. Применение низкотемпературного отжига после спекания методом ИПС позволило снизить сопротивление границ зерна на 1/3 при незначительном увеличении их среднего размера. Показано, что отжиг после ИПС является эффективным методом контроля качества границ зерен, размера зерна и плотности. Это позволяет повысить функциональные свойства твердого электролита SDC.

Ключевые слова: *твердый электролит, ионная (электрическая) проводимость, ИПС, отжиг после ИПС, граница зерна.*